Manuscript for consideration as an article at eLife

Geomagnetic and visual cues guide seasonal migratory orientation in the nocturnal fall armyworm, the world's most invasive insect

Yi-Bo Ma[1, †], Gui-Jun Wan[1, †], Yi Ji[1], Hui Chen[1,2], Bo-Ya Gao[1], Dai-Hong Yu[3], Eric J. Warrant[2], Yan Wu[4], Jason W. Chapman[1,5], Gao Hu[1,4 *]

1 State Key Laboratory of Agricultural and Forestry Biosecurity, College of Plant Protection, Nanjing Agricultural University, Nanjing 210095, China

2 Lund Vision Group, Department of Biology, Lund University, Sölvegatan 35, 22362 Lund, Sweden.

3 Plant Protection Station of Yuanjiang County, Yuanjiang 653399, China

4 Key Laboratory of Surveillance and Management of Invasive Alien Species, Guizhou Education Department, Department of Biology and Engineering of Environment, Guiyang University, Guiyang 550005, China.

5 Centre for Ecology and Conservation, University of Exeter, Penryn, Cornwall TR10 9FE, United Kingdom.

* *Correspondence to: Gao HU, 1 Weigang Road, Nanjing 210095, China. E-mail: hugao@njau.edu.cn*

† These authors have contributed equally to this work

Abstract

The mechanisms guiding nocturnal insect migration remain poorly understood. Although many species are thought to use the geomagnetic field, the sensory basis of magnetic orientation in insects has yet to be clarified. We developed an indoor experimental system to investigate the integration of geomagnetic and visual cues in the seasonal orientation of a globally distributed pest moth, the fall armyworm (*Spodoptera frugiperda*), a highly invasive species which in the past decade has colonized almost all potentially habitable regions of the globe. Our results demonstrate that fall armyworms require both geomagnetic and visual cues for accurate migratory orientation, with visual cues being indispensable for magnetic orientation. When visual and geomagnetic cues are placed in conflict moths become disoriented, although not immediately, indicating that sensory recognition of the conflict requires time to process. We also show that the absence of visual cues leads to a significant loss of flight stability, which likely explains the disruption in orientation. Our findings highlight that visual cues are critical for stable magnetic orientation in the fall armyworm, offering a basis for future investigations of visual-magnetic integration in noctuid migrants.

Introduction

Numerous species of larger nocturnal moths, particularly in the family Noctuidae (hereafter 'noctuid moths'), undertake long-distance multigenerational migrations in the Northern Hemisphere. Every spring across North America and Eurasia, billions of noctuid moths move hundreds of kilometers northwards to summer breeding grounds in the temperate zone, and in the subsequent fall their progeny return southward to lower latitude wintering areas (Holland et al., 2006; Satterfield et al., 2020; Hu et al., 2016, 2025; Huang et al., 2024). These migrations take place almost exclusively high above the ground, where fast winds facilitate rapid windborne transport leading to population redistribution over long distances (Chapman et al., 2010, 2015; Hu et al., 2016; Huang et al., 2024). Some of the most abundant species involved in these migrations are the world's most destructive agricultural pests, and thus they are of huge importance for food security and economic prosperity (Bauer & Hoye, 2014; Satterfield et al., 2020; Guo et al., 2020; Hu et al., 2025). It is thus of paramount importance to understand all aspects of the migratory patterns of noctuid moths.

Tracking the seasonal progression of resources requires noctuid moths to move in the appropriate direction (northwards in spring and southwards in fall), a process entailing three linked steps. Firstly, they determine the seasonally appropriate direction (north or south) in which to travel. Secondly, high-flying noctuid moths select

transporting winds that are broadly aligned with this direction. Thirdly, they adopt self-powered flight headings which are more-or-less aligned with the wind but, when required, offset to some degree to correct for crosswind drift (Chapman et al., 2015; Hu et al., 2016). Each step requires use of one or more compass senses based on globally stable cues to determine the required direction and behavioral responses (Mouritsen, 2018).

However, migration at night poses a considerable navigational challenge for noctuid moths and other night-flying insects (Warrant et al., 2011; Mouritsen, 2018; Foster et al., 2018; Gao et al., 2024; Grob et al., 2025). This is because they cannot rely on the sun for compass information in the way that diurnally migrating butterflies and hoverflies do (Mouritsen et al., 2002; Srygley et al., 2008; Gao et al., 2020; Massy et al., 2021; Pakhomov et al., 2025). Despite this challenge, radar, tagging, and tethered-flight studies demonstrate that many larger nocturnal moths are highly sophisticated navigators, capable of selecting and maintaining appropriate movement directions with a high degree of accuracy, even when flying high above the ground (Chapman et al., 2010; Dreyer et al., 2018ab; Menz et al., 2022; Chen et al., 2023; Dreyer et al., 2025). Their ability to achieve seasonally appropriate migration directions typically surpasses that of diurnal windborne insect migrants (Chapman et al., 2010; Hu et al., 2016; Werber et al., 2025), and even matches the capability of nocturnal songbird migrants (Alerstam et al., 2011, Chapman et al., 2016). Clearly, migratory noctuid moths must possess one or more accurate compass senses, but in all species but one, the source of the compass information has yet to be elucidated (Warrant et al., 2011; Foster et al., 2018; Mouritsen, 2018; Freas et al., 2023; Grob et al., 2025).

The one exception to this lack of knowledge of the sensory basis of navigation in noctuid moths is the Bogong moth (*Agrotis infusa*) of Australia, which uses both a magnetic compass integrated with visual cues (Dreyer et al., 2018a) and a stellar compass (Dreyer et al., 2025) to migrate in seasonally appropriate directions. The Bogong moth is unique, however, among long-range migratory noctuids because a single generation makes bidirectional movements to and from a highly restricted geographic location in southeast Australia (Warrant et al., 2016), rather akin to the migration of eastern North American monarch butterflies to and from a restricted area of central Mexico (Reppert et al., 2016). This is distinct from most other noctuid moth migrants, whose multigenerational migrations involve back-and-forth movements between broad latitudinal zones (Drake & Reynolds, 2012; Chapman et al., 2015; Gao et al., 2020; Tong et al., 2022; Hu et al., 2025) rather than to precise locations. Thus, other noctuid moths presumably do not require the same navigational precision and

may therefore be expected to have simpler sensory capabilities than the Bogong moth. We examine this question using the fall armyworm (*Spodoptera frugiperda*), one of the world's most serious crop pests, as a model for understanding general noctuid moth migration and navigation capabilities.

The fall armyworm is a migratory crop pest native to the Americas. It breeds year-round in tropical regions and annually migrates into temperate regions of North America (Nagoshi & Meagher, 2008; Westbrook et al., 2019). Over the past decade, the species has invaded and rapidly spread across Africa, Asia, and Australasia (Goergen et al., 2016; Kenis et al., 2023; Tay et al., 2023), assisted by its high migratory capacity (Chen et al., 2022, 2025; Gao et al., 2025). It now causes huge yield losses in these regions. In Southeast Asia and South China, fall armyworm populations breed year-round in tropical regions. Each spring, they migrate northward as far as Northeast China, and their progeny return southward in the fall after summer breeding (Li et al., 2020; Sun et al., 2021; Wu et al., 2021, 2022).

We recently found that fall armyworms from the year-round range in Southwest China (Yunnan) exhibit seasonally appropriate migratory headings when flown outdoors in virtual flight simulators: heading northward in the spring and southward in the fall. This seasonal reversal is controlled by photoperiod (Chen et al., 2023). However, the compass mechanism that fall armyworms use to select seasonally appropriate headings remains unknown. The Earth's geomagnetic field is a ubiquitous and reliable source of compass information (Mouritsen, 2018), and thus might be expected to be the primary compass cue used by night-flying migratory moths. However, despite intriguing indications of magnetoreception in the oriental armyworm, *Mythimna separata* (Xu et al., 2017), so far only the highly specialised Bogong moth has been demonstrated behaviorally to use magnetic information integrated with visual cues for orientation (Dreyer et al., 2018a, 2025).

To test whether more generalist noctuid moth migrants also rely on a magnetic compass for orientation, we investigated an invasive fall armyworm population in China using a newly developed tethered-flight assay designed to quantify migratory orientation (Fig. 1). While this indoor assay simplifies natural flight conditions, particularly due to the use of artificial visual cues, it provides a controlled framework for isolating the contributions of geomagnetic and visual cues. However, it should be noted that the setup does not include natural celestial cues, such as the moon, lunar polarization patterns, and stars, nor complex terrestrial topography, including mountains and water bodies, which could be incorporated in future studies to enhance

ecological relevance. Despite these limitations, the current assay represents an important first step towards understanding how these signals function under more realistic ecological conditions. The results of these experiments are not only of fundamental interest to sensory biology (Warrant & Dacke, 2011), but also have applied importance, given that the fall armyworm is one of the most mobile and invasive crop pests in the world (Kenis et al., 2023; Tay et al., 2023).

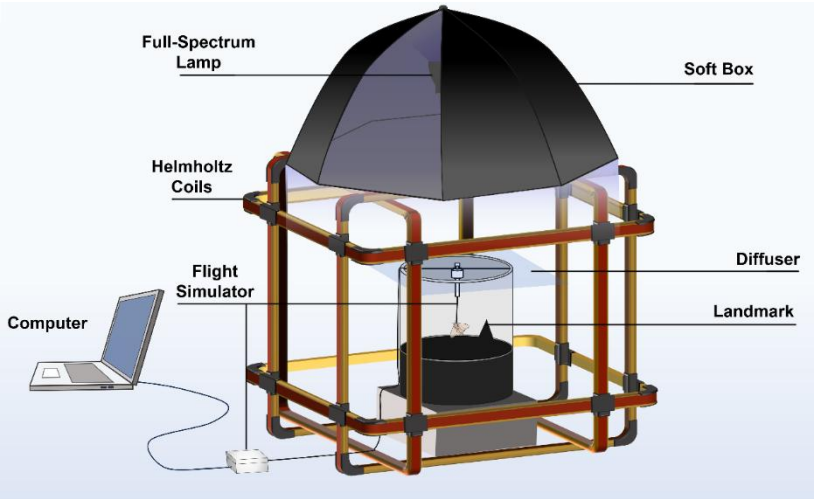

Fig. 1. Schematic of the experimental setup for studying magnetic orientation in fall armyworms. Moths are tethered to a vertical shaft at the center of the virtual flight simulator, with an encoder recording their flight heading. A full-spectrum lamp illuminates the arena, while the computer controlling the experiment is positioned outside the light field to avoid interference. Moths are free to rotate in any direction during the assay. Full experimental details in Methods. The cylinder is illustrated as clear in the figure to reveal the internal setup, but it is opaque in the actual experiment.

Results

Integration of geomagnetic and visual cues in the seasonal migratory orientation in a field population of fall armyworms

Previous studies have demonstrated that fall armyworms exhibit distinct season-specific orientation preferences under natural field conditions, however, it is important to note that, in the absence of tracking experiments, the actual migratory destination regions remain unknown. To examine if fall armyworms integrate geomagnetic and visual cues for seasonal migratory orientation, we measured flight responses of tethered moths within a virtual flight simulator (Dreyer et al., 2021) using a modified experimental approach used in Bogong moth studies (Dreyer et al., 2018a; Dreyer et al., 2025). The simulator consisted of a polyvinyl chloride (PVC) cylinder incorporating a visual cue on the side (a black triangle rising above a black horizon; Fig. 1). When

tethered within the simulator, the moth is restrained but is free to rotate and thus take up any orientation it chooses. The simulator was placed within a 3D Helmholtz coil system. Under control conditions, the coil was switched off, leaving the Earth's natural magnetic field (NMF) unaltered; under these conditions, magnetic north and geographic north were closely aligned. However, when the coils were switched on, they reversed the horizontal direction of the local magnetic field by 180° (the "Changed Magnetic Field", CMF) relative to the NMF, while maintaining constant field intensity and inclination angle (Fig. S1). Thus the field direction within the experimental arena temporarily switches so that its "local magnetic north" is aligned with geomagnetic south (GMS) and its "local magnetic south" is aligned with geomagnetic north (GMN), but all other field parameters remain constant. The experimental setup consisted of recording moth flight headings across five consecutive 5-minute phases (I, II, III, IV, V) of tethered flight under different experimental conditions that involved changing the azimuthal alignment of the visual cue and the local horizontal magnetic field component with respect to GMN and GMS (Fig. 2, Fig. S1). The assay was divided into these 5-min segments to provide the temporal resolution needed to detect changes in flight orientation as the relative alignment of magnetic and visual cues was systematically altered. In phases I and V moths were exposed to the NMF, whereas in phases II–IV moths were exposed to the CMF (Fig. 2). During spring migration trials, the visual cue was aligned with GMN (the expected migratory orientation in spring) at the start of the trial, whereas in fall migration trials the set-up was reversed, with the visual cue initially aligned with GMS (the expected migratory orientation in fall; Fig. 2).

The first two experiments involved a field population of moths (collected as late-instar larvae) tested during spring and fall migration periods (Figs. 2*A* and 2*B*). In phase I, the visual cue was aligned with the expected seasonal magnetic direction in the NMF, and moths exhibited significant group orientation towards the visual cue in both seasons (Spring: mean vector [MV] = 347.4° (95% CI: 319.5°, 16.71°), vector strength [R^*] = 1.59, $P < 0.001$, Fig. 2*A-I*; Fall: MV = 183.6° (95% CI:211°,162°), $R^* = 1.76$, $P < 0.001$; Fig. 2*B-I*). In phase II, the horizontal component of the geomagnetic field was rotated 180° (the CMF condition), creating a conflict between the visual cue direction and the expected magnetic orientation. Despite the shift in the magnetic field direction, moths continued to show significant group orientation toward the visual cue during this 5-minute period (Spring: MV = 319.1° (95% CI:351°,283°), $R^* = 1.39$, $P < 0.005$, Fig. 2*A-II*; Fall: MV = 191.0° (95% CI:235°,153°), $R^* = 1.16$, $P < 0.05$, Fig. 2*B-II*), indicating that, at least initially, the visual cue was dominant compared to the magnetic cue. During phase III, which was a second 5-minute period of the experimental conditions

applied in phase II, moths lost their significant group-level orientation in both seasons (Spring: $R^* = 0.67$, $P > 0.05$, Fig. 2*A-III*; Fall: $R^* = 0.34$, $P > 0.05$; Fig. 2*B-III*), indicating that over time they had become confused due to the conflicting nature of the cues. Although we did not analyze flight activity level due to technical limitations, the loss of group orientation is unlikely to be attributable to a decline in the moths' motivation to maintain orientation during prolonged flight in the simplified experimental environment, as the Rayleigh test showed no significant differences in the *r*-values of individual flight vectors across phases I–III (Figs. 2*A* and 2*B*; Table S2; Table S3). In phase IV, the visual cue was realigned with the expected seasonal magnetic orientation, but this time in the CMF (i.e., the cues were arranged in the same way as in phase I but rotated by 180°). Therefore, the moths should not be able to distinguish between phase I and phase IV and thus are expected to show the same orientation response in both phases. Indeed, the moths tended to show group orientation towards the congruent cues once again, albeit not quite reaching significance in spring (Spring: MV = 245.2° (95% CI: 193.2°, 309.4°), $R^* = 0.95$, $0.05 < P < 0.10$, Fig. 2*A-IV*; Fall: MV = 354.3° (95% CI: 331.4°, 27.2°), $R^* = 1.49$, $P < 0.005$; Fig 2*B-IV*). Finally, in phase V, the initial configuration was restored, and moths regained significant group orientation toward the congruent visual cue and the expected magnetic orientation in the NMF (Spring: MV = 343.8° (95% CI: 326.56°, 2.92°), $R^* = 1.84$, $P < 0.001$, Fig. 2*A-V*; Fall: MV = 167.7° (95% CI: 191°, 146°), $R^* = 1.62$, $P < 0.001$, Fig 2*B-V*). These results demonstrate that fall armyworm integrates geomagnetic field information with visual cues to achieve stable orientation. However, when geomagnetic and visual cues do not align with expected seasonal directions, moths gradually lose orientation, reinforcing the critical role of cue integration in maintaining migratory stability.

Integration of geomagnetic and visual cues is consistent in laboratory-reared fall armyworms

Our previous research showed that fall armyworms reared under artificially simulated fall migratory season and tested indoors with optic flow and starry sky projections exhibited southward orientation in a flight simulator, consistent with the behavior observed in wild individuals tested outdoors under natural night skies (Chen et al., 2023). To determine whether lab-raised moths exposed to simulated seasonal photoperiods respond the same way to geomagnetic and visual cues, we tested a population reared under a simulated fall photoperiod in the same experimental setup as that of the field population fall group (Fig. 2*C*). The results closely matched those from the field population (Fig. 2*B*). In phase I, with visual cues aligned to GMS in the NMF, lab-raised moths oriented significantly southward (MV = 182.9° (95% CI: 203°,

156°), $R^* = 1.77$, $P < 0.001$, Fig. 2*C-I*). When the geomagnetic field was reversed (CMF), moths initially orientated towards the visual cue, showing no immediate response to the shifted field (MV = 184.9° (95% CI: 222°, 153°), $R^* = 1.31$, $P < 0.05$, Fig. 2*C-II*). After an additional 5-minute period without changes, significant group-level orientation was lost ($R^* = 0.69$, $P > 0.05$, Fig. 2*C-III*). When the visual cue was realigned with the changed GMS, significant orientation was restored (MV = 4.1° (95% CI: 350.7°, 19.3°), $R^* = 2.17$, $P < 0.001$, Fig. 2*C-IV*), though the direction was opposite that in phase I. Finally, returning to the original setup restored the initial orientation pattern (MV = 137.6° (95% CI: 189.9°, 94.9°), $R^* = 1.04$, $P < 0.05$, Fig. 2*C-V*). These results demonstrate that lab-raised fall armyworms integrate geomagnetic and visual cues similarly to field populations, emphasizing the role of photoperiod during development in shaping seasonal multimodal migratory orientation.

To confirm that the loss of orientation in experimental groups was due to the cue conflict rather than diminished motivation to maintain orientation arising from a prolonged test duration, we conducted a control experiment with the lab-raised simulated fall population, where the visual cue and GMS remained consistently aligned. In this group, moths maintained significant orientation in their expected migratory direction throughout the experiment when exposed to congruently-aligned cues, irrespective of whether under NMF or CMF conditions (Fig. 2*D*; directional statistics in Table S1). This confirms that the loss of orientation observed in experimental groups was driven by misalignment between visual and geomagnetic cues.

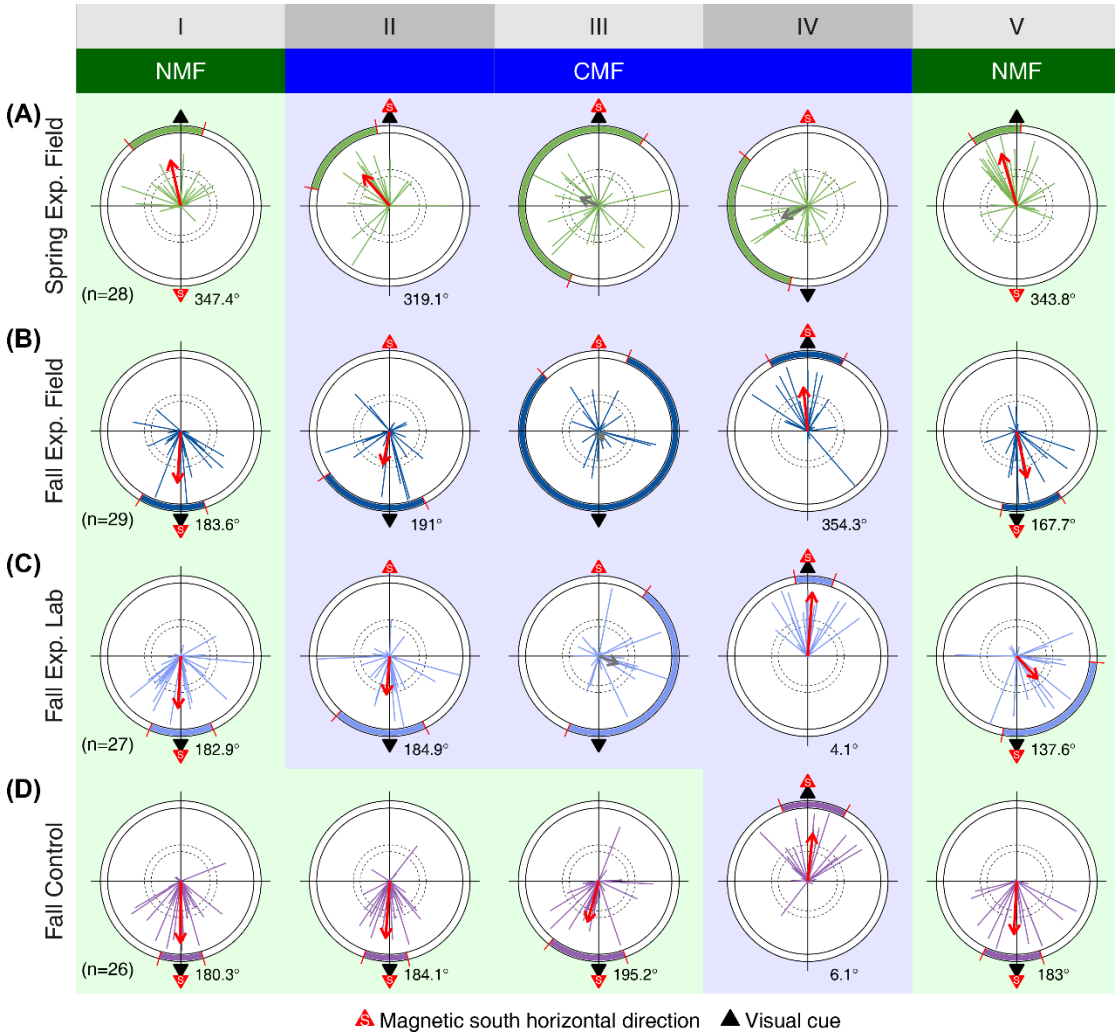

Fig. 2 The Earth's magnetic field and visual cues guide migratory flight behavior in both a field population and lab-raised fall armyworms. (*A*) Flight orientation behavior of a spring field population of moths ("Spring Exp. Field") in response to visual and geomagnetic cues. (*B*) Flight orientation behavior of a fall field population of moths ("Fall Exp. Field") in response to visual and geomagnetic cues. (*C*) Flight orientation behavior of lab-raised fall-conditioned moths ("Fall Exp. Lab") in response to visual and geomagnetic cues. (*D*) Flight orientation behavior of lab-raised control fall-conditioned moths ("Fall Control"), tested with consistent visual and geomagnetic alignment. For simplicity and consistency, we tested only conditions in which the visual cue pointed in the putative migratory direction, coinciding with magnetic north in spring and with magnetic south in fall. The putative migratory direction was defined based on the seasonally different orientation directions revealed by our previous field experiments (Chen et al., 2023). Each group underwent five sequential 5-minute phases (I–V), with each subplot representing individual moths' flight directions in the simulator. The length of each vector represents individual directedness (r), ranging from 0 to 1, where the outer edge of the plot corresponds to $r = 1$. The thick mean vector (MV) arrow represents the weighted average of individual orientations, calculated

using Moore's modified Rayleigh test (see Methods), and is red when there is significant group orientation but grey when it is not significant. The R^* value quantifies the directedness of the MV. Dashed circles indicate thresholds for statistical significance, with radii corresponding to $P < 0.05$ and $P < 0.01$. Shaded sections of the outer diameters of the circles represent the 95% confidence limits of the group orientation. The outermost radius represents $R^* = 2.5$. The black triangle denotes the position of the visual cue, while the red triangle indicates the direction of the expected migratory orientation in each season (north in spring, south in fall). The experimental setup included both the natural magnetic field (NMF, panels with light green background) and a changed magnetic field (CMF, panels with light blue background) where the horizontal magnetic field direction was reversed; further details of the magnetic field parameters in the NMF and CMF are shown in Fig. S1.

Fall armyworms show a delayed response to changes in magnetic fields

Our results show that migratory fall armyworms rely on both the Earth's magnetic field and visual cues to determine their flight direction. However, for moths to maintain constant orientation, the two sensory inputs must remain congruent, and when they come into conflict the moths become disoriented at the group level (but not at the individual level; Fig. 2). Notably, this response to the conflict between visual and geomagnetic cues was not instanteous but delayed until the second 5-minute experimental phase with this condition, consistent with similar results from Bogong moths (Dreyer et al., 2018a). Initial analyses using a 5-minute resolution provided limited temporal detail. To improve resolution, we subdivided each 5-minute phase into ten 30-second intervals and independently analyzed directional consistency using Moore's Rayleigh test to calculate the R^* for each 30-second period (Fig. 3).

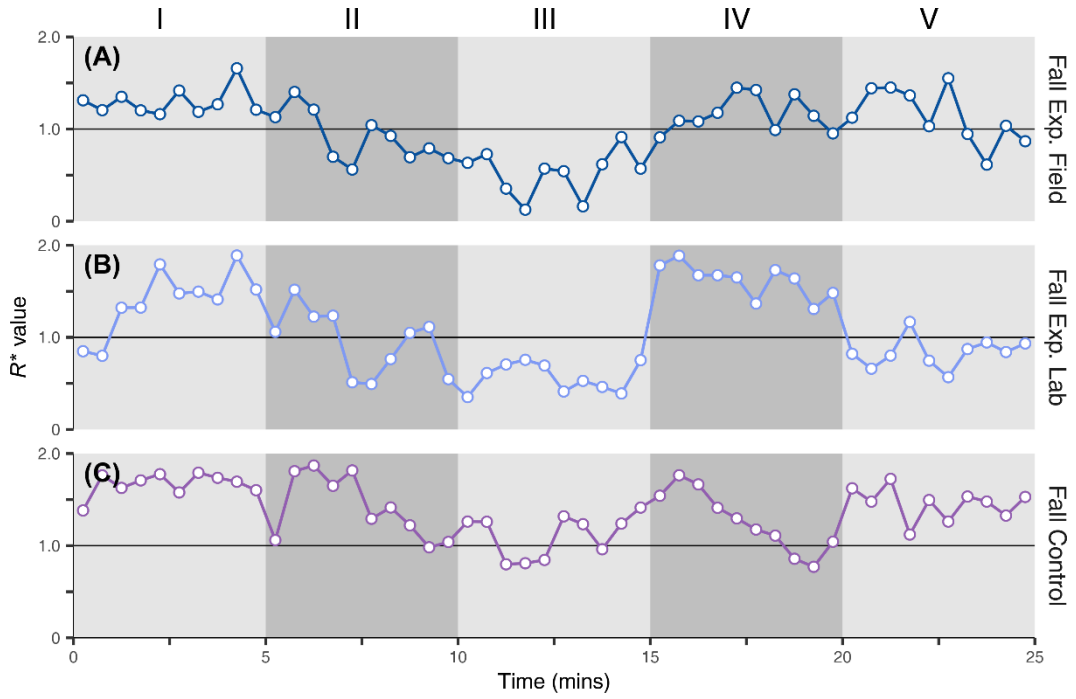

Fig. 3. Fall armyworms exhibit a delayed response to changes in magnetic-visual cue alignment. The behavioral data for (*A*) fall field population experimental ("Fall Exp. Field", data from Fig. 2B), (*B*) fall lab-raised experimental ("Fall Exp. Lab", data from Fig. 2C), and (*C*) fall lab-raised control ("Fall Control", data from Fig. 2D) groups were analyzed in 30-second time bins, resulting in ten bins over each 5-minute phase of the experiment. For each group, Moore's modified Rayleigh test was applied, and the obtained R^* values were plotted against time. $R^* > 1$ indicates a significant collective orientation within that 30-second interval, while $R^* < 1$ indicates the absence of significant group-level orientation.

During phase I, R^* values in both experimental groups remained >1 (Figs. 3*A-I* and 3*B-I*), indicating significant orientation behavior. When the magnetic field was rotated to conflict with visual cue directions, R^* values did not drop immediately but instead declined gradually over time (Figs. 3*A-II* and 3*B-II*). By phase III, R^* values were consistently <1, indicating a loss of significant orientation (Figs. 3 *A-III* and 3 *B-III*). Upon realigning the magnetic field with visual cues, R^* values showed a gradual increase, eventually exceeding 1 in both groups (Figs. 3*A-IV* and 3*B-IV*). When the original configuration was restored, the field population group consistently exhibited R^* values above 1 (Fig. 3*A-V*), while the lab-raised group had R^* values hovering around 1 (Fig. 3*B-V*). These results indicate that fall armyworms require time to resolve conflicting navigational inputs before losing group orientation entirely, or to react to congruent cues and regain group orientation. In the lab-raised control group, where the geomagnetic field and visual cues remained consistently aligned, R^* values consistently remained above 1 (Fig. 3*C*), confirming that the decline in group-level orientation observed in the experimental groups was driven by conflicts between

geomagnetic and visual cues, mirroring the results found in Bogong moths (Dreyer et al., 2018a).

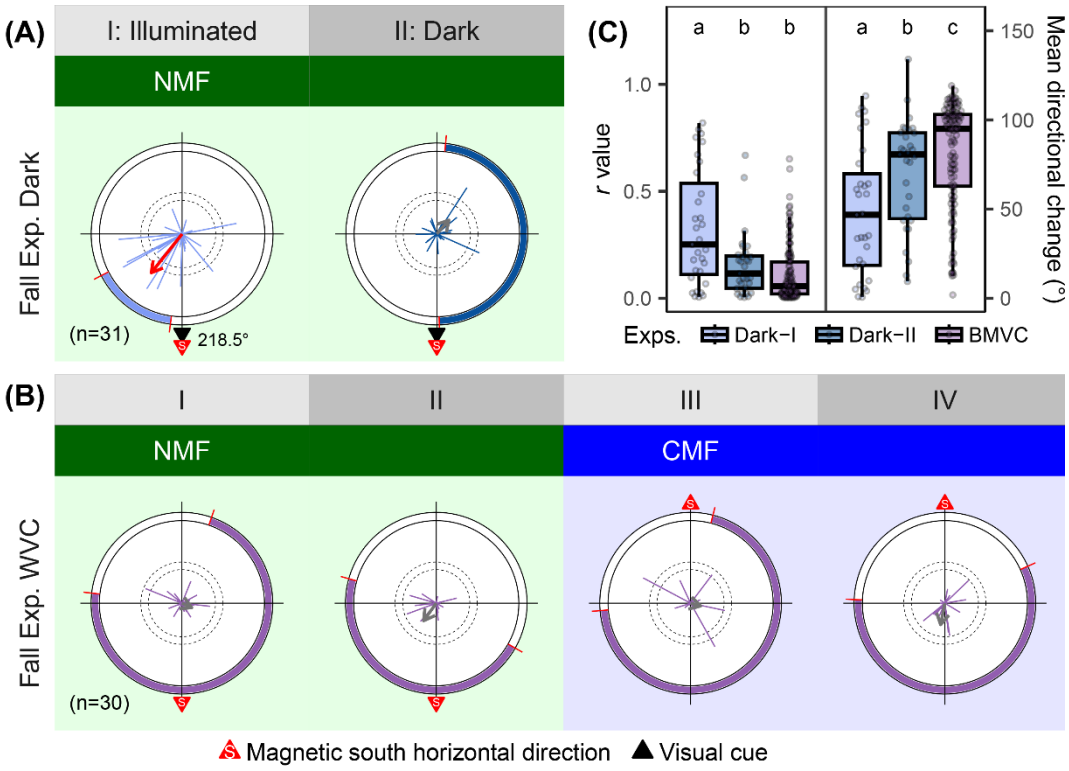

Fig. 4. Visual information is essential for maintaining group flight orientation in fall armyworms. (*A*) The lab-raised, fall-conditioned population lost significant group orientation under complete darkness ("Fall Exp. Dark"). (*B*) The lab-raised, fall-conditioned population exhibited a significant loss of group orientation under illuminated conditions where visual cues were reduced to the bare minimum ("Fall Exp. BMVC"), i.e., obvious visual cues such as the black triangle shown in Fig. 1 were not provided; however, because the experiments were conducted under illuminated conditions, complete elimination of all visual information is impossible. (*C*) The distribution of Rayleigh test *r*-values for individual moth orientations across different treatment groups (*Left*), and the distribution of average directional change per second (*Right*), the latter reflecting flight stability. The box plots represent the interquartile range (IQR), with the horizontal line inside indicating the median. Whiskers extend to the most extreme data points within 1.5 times the IQR. Pairwise comparisons of the *r*-values were performed using the Wilcoxon rank-sum test and Wilcoxon signed-rank test (The Wilcoxon signed-rank test is only used to compare non-independent (i.e., paired or related) samples. For more information, please refer to the Statistical Analysis section). Multiple comparisons were corrected by the Benjamini-Hochberg method. Detailed statistical results are provided in Table S4. Comparisons of the average directional change per second were performed using the same method as that used for r-values, with statistical results provided in Table S5. Groups labeled with different

337 letters differ significantly ($P < 0.05$). We also analyzed the *r*-values and average directional
338 change per second in the Fall Exp. Field, Fall Exp. Lab, Exp. Fall Control, and the
339 experiment shown in this figure, with results consistent with those shown here (see Tables
340 S4 and S5, Fig. S4).

341 **Visual cues are essential for magnetic orientation in fall armyworms**

342 Growing evidence supports the idea that geomagnetic cues provide essential compass
343 information for orientation across a broad range of taxa, supporting diverse
344 navigational tasks (Mouritsen, 2018; Dreyer et al.,2018a; Fleischmann et al., 2018;
345 Wan et al., 2021; Grob et al., 2024; Goforth et al., 2025). To determine whether
346 geomagnetic input alone is sufficient for flight orientation in fall armyworms, we
347 conducted a series of experiments to evaluate the role of visual cues in their orientation
348 behavior. In particular, we examined whether these moths could maintain orientation
349 in the absence of visual cues.

350 As a control, we first tested lab-raised, fall-conditioned moths in an arena where visual
351 landmarks were aligned with GMS in the NMF (Fig. 4*A*). When illuminated, moths
352 showed significant group orientation towards the visual cue (MV = 218.48° (95% CI:
353 242°, 187°), $R^* = 1.50$, $P < 0.005$, Fig. 4*A-I*), consistent with our previous results (Fig.
354 2*B*). To determine whether moths could maintain orientation without visual information,
355 we then removed all light sources, allowing moths to continue flying in total darkness.
356 Under these conditions, moths lost significant group-level orientation ($R^* = 0.5$, $P >$
357 0.05, Fig. 4*A-II*), suggesting that their orientation behavior is dependent on the
358 presence of light. The loss of orientation may be due to the absence of usable visual
359 landmarks, or the lack of light in a dark environment causing the moths to lose their
360 sense of direction. However, it is still unclear how the absence of usable visual
361 landmarks in non-dark environments would affect the moths' orientation behavior.

362 To further investigate this, we tested a lab-raised, fall-conditioned population of moths
363 in a simulator, primarily to determine whether moths could maintain orientation under
364 illuminated conditions where visual cues on the interior walls of the cylindrical flight
365 arena were minimized. In this experiment, we provided a uniform visual environment
366 (i.e., under illuminated conditions, visual cues were not provided on the interior walls
367 of the cylindrical flight arena). After recording 10 minutes of orientation behavior under
368 the NMF, we reversed the horizontal component of the geomagnetic field using
369 Helmholtz coils (CMF) and recorded their flight orientation for an additional 10 minutes.
370 Despite the altered magnetic field direction and sufficient time for adaptation, moths
371 exhibited no significant group orientation across all four testing phases (Fig. 4*B*;

directional statistics in Table S1). The lack of group-level orientation under near-uniform visual conditions suggests two possibilities: individual moths may have maintained stable flight, but due to the absence of reliable orientation cues, their group-level directional choices were random; or their flight may have been unstable, making it difficult to assess individual orientation behavior. We first compared the differences in the Rayleigh test *r*-values of moths across different experimental phases (Fig. 4*C*, *Left*), using the Wilcoxon signed-rank test for the non-independent Fall Exp and Fall Dark groups, and the Wilcoxon rank-sum test for all other independent group comparisons. This is because the Rayleigh test evaluates the concentration of data, with an *r*-value close to 1 indicating highly consistent flight directions, and close to 0 suggesting more random flight directions. The results showed that under conditions with visual cues (Fall Exp. Dark-I), moths had significantly higher *r*-values compared to conditions of complete darkness (Fall Exp. Dark-II) or visual cues reduced to the bare minimum (Fall Exp. BMVC).

We also considered the limitations of the Rayleigh test, as its *r*-value only reflects the overall directional tendency and does not reveal real-time flight stability. For example, a moth exhibiting two stable flight phases, one oriented north and the other south, would yield a low *r*-value despite maintaining stability within each phase. Conversely, a moth losing flight stability could also produce a low *r*-value, making it difficult to distinguish between these two scenarios based on *r*-value alone. Therefore, we introduced the analysis of per-second angular change (Fig. 4*C*, *Right*) to assess dynamic fluctuations in flight behavior, providing a clearer understanding of whether the observed differences in *r*-values were due to stable orientation or a loss of flight control. Our analysis showed that the experimental groups tested under conditions lacking visual cues exhibited significantly lower flight stability than the other experimental groups (Fig.4C; Fig. S4). This conclusion is similar with the earlier analysis based on individual Rayleigh test *r*-values (Fig. 4C). Moths in these conditions exhibited significantly higher angular change rates, suggesting that the reduced stability likely contributed to the lower directedness, as indicated by the reduced vector lengths (*r*). Notably, even though a small subset of individuals in these groups managed to sustain stable flight, their directional choices appeared random rather than goal-oriented (Figs. 4*A*-*II* and 4*B*).

Discussion

The integration of geomagnetic and visual cues for flight orientation has so far been experimentally demonstrated only in the Australian Bogong moth, a species

undertaking a precisely oriented, long-distance round-trip migration to and from a highly restricted aestivation site within a single generation (Dreyer et al., 2018a). Although this life-history strategy is uncommon among migratory insects, our development of an indoor behavioral paradigm in the fall armyworm, a globally distributed nocturnal migratory insect with multi-generational and partially migratory patterns in China, extends this dual-cue orientation strategy to a species exhibiting a migratory ecology more typical of insects in general. These findings demonstrate that this orientation mechanism is not unique to the Bogong moth and may instead represent a conserved orientation mechanism broadly employed across migratory moth species, though additional species will need to be evaluated to demonstrate this. Crucially, we show that visual cues are indispensable for magnetic orientation in the fall armyworm, as directional responses disappeared in the absence of structured visual input. Furthermore, our findings reinforce recent results on seasonal shifts in orientation behavior in this species (Chen et al., 2023), highlighting the ecological relevance of this guidance system.

Our findings thus emphasize the importance of integrating multiple cues for successful orientation. It is often assumed that animals lack magnetic orientation capabilities if they fail to orient under changes in the geomagnetic field (Pakhomov et al., 2025), either in appropriate lighting conditions or in darkness, without additional cues. However, our study demonstrates that the absence of group seasonal orientation under geomagnetic fields, in full-spectrum light or in darkness, does not preclude magnetic orientation when additional sensory cues are integrated. Specifically, in the Northern Hemisphere, a magnetic compass provides global directional cues for fall armyworms, enabling them to align magnetic north (or magnetic pole) and south (or magnetic equator) with visual cues during spring and fall, respectively, to facilitate seasonal orientation—a hallmark of annual long-distance migration in migratory species. Although the magnetic compass is critical, as evidenced by the loss of group orientation when the horizontal geomagnetic field was reversed while intensity and inclination remained unchanged, our results reveal that magnetic orientation cannot occur without appropriate visual cues. We also show that the loss of flight stability observed when visual cues are minimal is likely a major cause of the lack of group magnetic orientation. This highlights the complexity of magnetic orientation strategies in nocturnal migratory insects, emphasizing the crucial interaction between the magnetic compass and visual navigation systems. Further investigation by altering the geomagnetic polarity and vertical geomagnetic component is required to determine whether the magnetic compass guiding seasonal orientation in nocturnal migratory fall

armyworms is polarity-sensitive, inclination-sensitive, or both; a factor which is pivotal to understanding the biophysical mechanisms underlying magnetoreception (Mouritsen, 2018; Hore et al., 2016; Grob et al., 2024).

Desert ants and Bogong moths have also been shown to integrate geomagnetic and visual cues for navigation. Desert ants rely on a magnetic compass during look-back-to-the-nest behavior, combining magnetic cues with local visual landmarks, such as their nest (Grob et al., 2024). In contrast, Bogong moths have been demonstrated to integrate global stellar cues with the Earth's magnetic field for orientation (Dreyer et al., 2025). Like Bogong moths, fall armyworms can migrate hundreds, or even thousands, of kilometers over several successive nights (Warrant et al., 2016; Li et al., 2020). Recent work on skyglow has shown that large-scale nocturnal luminance gradients can bias the orientation of fall armyworm moths, with individuals tending to orient towards darker regions of the sky (Ji et al., 2025). However, whether fall armyworms are capable of detecting and exploiting naturally occurring light-dark gradients, such as those generated by the Milky Way, for orientation under natural conditions remains unknown.

Under natural migratory conditions, fall armyworms are unlikely to experience a visual environment dominated by only a single, static, and highly salient landmark. Celestial cues are intermittently available, and local features shift during flight. Given this complexity, several key questions about orientation in fall armyworms remain unresolved. (a) One important issue is the role of celestial cues when local landmarks are absent. Experimental disruptions to local features could test whether celestial cues, such as those from the moon or stars, can compensate for the absence of local landmarks. (b) When multiple visual cues are available, it is essential to understand how they are weighted and integrated with geomagnetic information. To explore this, experiments could vary the presence and prominence of different visual cues (e.g., celestial cues vs. local landmarks) and examine how they interact with geomagnetic information to guide orientation. (c) Transient visual cues, such as shifting clouds or changing lighting conditions, may also influence orientation. Experiments could simulate these transient cues and assess how they affect orientation, both in isolation and in conjunction with geomagnetic cues. (d) Finally, given that luminance gradients are unlikely to be absent in natural nocturnal environments, how such visual cues may be integrated with the geomagnetic field for orientation remains a critical topic for future research. To investigate this, studies could manipulate luminance gradient strength and stability, and test how these gradients interact with geomagnetic cues to influence orientation, further advancing our understanding of the integration of visual and

geomagnetic cues during nocturnal migration.

In conclusion, our findings underscore the indispensability of visual cues in facilitating seasonal magnetic orientation. To date, comparable results have been demonstrated only in another nocturnal moth, the Bogong moth (Dreyer et al., 2018a). Unlike many vertebrate studies, in which behavioral changes can be induced by magnetic field manipulations alone under simplified conditions (Mouritsen, 2018; Burda et al.,1990), these findings highlight the complex, multimodal nature of navigation in nocturnal migratory insects, as well as the methodological considerations associated with studying their orientation behavior. This work advances our understanding of migratory orientation strategies and raises the possibility that similar magnetic-visual integration mechanisms may be shared among long-distance migratory moths. Furthermore, the application of genome editing in fall armyworms, combined with the indoor behavioral paradigm developed here, provides a promising avenue for dissecting the molecular basis of magnetoreception and the interplay between sensory systems.

Methods

Field population

All wild populations used in this study were collected from farmland in Yuanjiang Hani and Yi Autonomous County, Yunnan Province, a region primarily characterized by maize cultivation. Fall-generation populations were collected during September to October of 2023 and 2024, while spring-generation populations were collected from April to May in 2024, as mature larvae at the 5th to 6th instar stages. Each larva was individually collected and reared in a cylindrical container, fed with fresh maize leaves from the collection site until pupation. Upon pupation, larvae were transferred to transparent, thin plastic cups sealed with plastic film. A cotton ball moistened with water was placed in each cup to maintain adequate humidity during the pupal stage. After eclosion, adults were individually provided with a 10% honey solution. All experimental individuals were reared at the Yuanjiang Plant Protection Station, a facility located near agricultural fields and well isolated from urban light pollution. To maintain natural environmental conditions, all electrical devices were strictly excluded from the facility, and windows were kept open around the clock to allow for natural light cycles and ambient temperature conditions.

Lab-raised population

The laboratory-reared population of the fall armyworm used in this study was primarily derived from wild individuals collected from a maize field in Yuanjiang, Yunnan

Province (Google Maps coordinates: 23.604°N, 101.977°E) during October to November 2022, with the exception of individuals used in experiments Fall Exp. Dark and Fall Exp. BMVC (see Fig. 4), which were collected from the same field location during October to November 2024. All experiments were conducted using individuals from the 3rd to 5th laboratory-reared generations. The Fall Exp. lab and fall control populations were reared from January to May 2023, whereas the Fall Exp. Dark and Fall Exp. BMVC populations were reared from January to February 2024.

For behavioral assays conducted under ambient temperature conditions, a programmed photoperiodic regimen was implemented to simulate the seasonal changes in day length typical of autumn in East Asia. All treatments were maintained at a constant temperature of 27 ± 1°C and a relative humidity of 60% ± 5%. In the fall photoperiod treatment, the initial light cycle at egg hatching was set to 13 hours of light and 11 hours of darkness (13L:11D), followed by a daily reduction of 2 minutes in the light period. By the time adult moths emerged and were subjected to experimental testing approximately one month later, the photoperiod had been adjusted to approximately 12L:12D.

Attachment of tethering stalks on moths

We used the same method for the attachment of tethering stalks on moths as in the previous study on fall armyworm moth orientation (Chen et al. 2023). Prior to tethering, unmated 2-day-old adult moths were housed in plastic cups and sedated at 4°C for at least 1 minute to facilitate handling. The moths were then transferred to an operational platform, where scales were carefully removed from the junction of the dorsal thorax and abdomen to ensure secure attachment. The tether consisted of a slender, non-magnetic copper stalk measuring 0.75 mm in diameter and approximately 2 cm in length. The terminal end of the stalk was bent into a fork-like structure, which was carefully affixed to the prepared thoracic-abdominal junction using Pattex PSK12CT-2 glue. To maintain consistency, this standardized tethering method was applied uniformly across all experimental protocols.

Behavioral apparatus

Our flight simulator system is consistent with the one used in previous research on fall armyworm (Chen et al., 2023), utilizing the Flash flight simulator system. This system was developed based on the early design of the Mouritsen-Frost flight simulator, was developed with a more user-friendly human–machine interaction interface and an integrated optic-flow system (Flash Flight Simulator Data Acquisition System.exe is

available on Mendeley Data: https://doi.org/10.17632/6jkvpybswd.1). and adapted for our experiments conducted in Yuanjiang (longitude 101.98°E, latitude 23.60°N). However, in contrast to previous studies, we did not include optic flow in order to avoid introducing additional visual complexity. The moths are able to freely rotate on the horizontal plane within the simulator, with their azimuth measured by an encoder system with a resolution of 0.9°. The flight direction (relative to magnetic north) is recorded in real time by the Flash flight simulator data acquisition system developed by Hui Chen, and the data is saved as angle values in a text file. In our experiments, the encoder (made of non-magnetic materials) samples the azimuth five times per second and is equipped with a graphical interface, which allows for continuous monitoring of the moth's azimuth and flight status to reconstruct the flight path. The encoder is connected to the axis that holds the moth, with the axis measuring 15 cm in length and 1 mm in diameter, made of carbon fiber material and wrapped in a carbon fiber tube to protect its structure.

The arena consists of an opaque PVC cylinder with a diameter of 400 mm, a height of 500 mm, and a thickness of 5 mm as the main structure, surrounded by white wallpaper, with a 20 cm high black wallpaper strip at the bottom simulating the horizon. A visual cue is provided by a black isosceles triangle (10 cm high, 10 cm base) made from black wallpaper and fixed to the horizon at the bottom of the arena. The entire arena is placed on a square wooden board with a side length of 50 cm and a thickness of 1 cm, covered with black blackout cloth. The bottom of the wooden board is equipped with a plastic base to reduce friction, ensuring that the arena can rotate smoothly and quickly during the experiment, changing the direction of the visual cues while avoiding interference with the moth's activity.

In the BMVC experiment, we used an opaque white acrylic cylinder with the same dimensions as the PVC cylinder as the arena. No modifications were made to the interior of the arena, primarily because the interior of the white acrylic cylinder is smooth and uniform enough, and any additional treatment could potentially introduce noticeable visual cues. We also removed the carbon fiber crossbar used to fix the simulator and instead fixed it directly to the top acrylic cover to further minimize potential visual cues that the moth might use. Our goal was to minimize the visual cues available to the moth as much as possible, rather than attempting to completely eliminate all visual cues.

A DH1766-series linear, three-channel, programmable DC power supply (Beijing Dahua Radio Instrument Factory, China) with adjustable current and voltage was used

to power the full-spectrum LED employed in the experiments. The light source was enclosed within a 90 cm diameter GODOX softbox to ensure even distribution of light within the experimental arena. The softbox is fixed to a Helmholtz coil, with the flight simulator located at its center. The top of the arena is equipped with a UV-transmitting acrylic panel and covered with Lee Filters 250 semi-white diffusion paper to control the amount of light transmitted. Spectral measurements, which include both spectral irradiance and composition, were taken at the position corresponding to the moth's head using an ATP2000P spectrometer (Optosky Technology Co. Ltd., Xiamen, China), ensuring consistent lighting conditions across all visual treatments (see Fig. S3). The ambient light level in the experimental environment was measured to be below 1 lux using a Testo 540 lux meter (Testo SE & Co. KGaA, Titisee-Neustadt, Germany). Further work is still required to compare the illuminance used in this study with that under natural conditions, which are inherently variable.

Artificial simulation of the Earth's magnetic field

A three-dimensional pair of Helmholtz coils (Nanjing Science Sky Technology Limited) was used to manipulate the Earth's magnetic field. The coils measured 1200 × 1100 × 1000 mm, with a cold-state direct current resistance of 2Ω per coil and an insulation resistance exceeding 10MΩ. The magnetic field strength at the central X, Y, and Z axes exceeded 10 GS@6A (maximum current), with a spatial uniformity of 0.5% within a φ 144 × 144 × 144 mm volume. At the start of each experiment, we used a TM4300B handheld three-axis fluxgate magnetometer to measure the ambient magnetic field strength and spatial vector intensity at the experimental site (averaged over three measurements). A DH1766 series linear three channel output precision programmable DC power supply (Beijing Dahua Radio Instrument Factory, China) with adjustable current and voltage was employed to apply a controlled current to the 3D Helmholtz coils, reversing the horizontal geomagnetic component by approximately 180°. Crucially, we ensured that total magnetic field intensity (E), horizontal component intensity (H), and magnetic inclination angle (α) remained statistically unchanged between the controlled magnetic field (CMF) and the normal magnetic field (NMF) (see Fig. S1*A-D*). Electromagnetic noise at the experimental site was quantified by measuring the magnetic component of the time-dependent electromagnetic field across a 10 kHz resolution bandwidth. Measurements were performed using a Spectran NF-5035 spectrum analyzer (1 Hz-30 MHz, Aaronia AG) connected to an MDF-9400 magnetic-field antenna (9 kHz-400 MHz, Aaronia AG) via a UBBV-MDF960X preamplifier (9 kHz-60 MHz, 25 dB gain) and a 10-m RF cable. The

frequency range from 1 to 10 MHz was measured using the external antenna-preamplifier configuration, while low-frequency noise between 2 kHz and 1 MHz was measured using the internal magnetic probe of the spectrum analyzer. During each measurement session, the spectrum analyzer continuously scanned the frequency range for 40 minutes, and values were logged using the instrument's peak-hold mode. Pronounced noise peaks were detected in the 2 kHz-1 MHz range, whereas noise levels from 1 to 10 MHz were low and relatively stable, ranging between 0.01 and 0.001 nT with only minor fluctuations (see Fig. S1*E*).

Experimental procedure

The orientation experiment followed the protocols established in our previous study (Chen et al. 2023). Experiments began after complete darkness in the night sky: the field population were tested after adapting to the natural dark environment for at least 60 minutes, while the lab-raised population started after adapting to the dark environment for at least 60 minutes following the light-to-dark cycle switch in the incubator, in a laboratory away from large electrical equipment, artificial noise, plants, and other potential sources of interference. The computer screen was positioned away from and facing away from the experimental setup. Weak red light was used only when attaching the tethering stalks and fixing the moth to the simulator. After the moth was fixed, a waiting period of 20 to 30 seconds was allowed for the subject to stabilize before data recording began. During this process, it was verified whether the insect could switch between clockwise and counterclockwise rotations. If the insect rotated in only one direction and could not fly stably, no further experiment was conducted. The encoder's horizontal placement was also checked to ensure it was not affected by tilting. The moth's wing vibrations were confirmed to be strong, with equal amplitude on both wings (indicating that the contact glue did not interfere with the wings). During the experiment, the insect's flight state was monitored by observing fluctuations in the pointer values on the experimental software. If the values did not change within 10 seconds, the experimenter needed to approach the flight arena and listen for any sounds of wing vibrations. If the insect stopped flying, the experimenter gently tapped the wall to stimulate the insect to continue flying. We analyzed individuals that were able to maintain fewer than four instances of wingbeats cessation during the experiment.

Statistical analysis

All statistical analyses and graph generation were performed using R (version 4.1.3), accessible at https://www.r-project.org/. A custom R script, incorporating bootstrap

confidence intervals, was used for Moore's Modified Rayleigh Test (MMRT) — a non-parametric test increasingly applied in orientation behavior studies (Massy et al., 2021; Chen et al. 2023), the script is available on: https://doi.org/10.1098/rspb.2021.1805. MMRT accounts for both mean directions and directedness (vector lengths) of individuals, making it an alternative to the Rayleigh test. MMRT assesses whether a group exhibits significant directional tendencies, using the parameter R^* (a scaled alternative to r in circular regression), which quantifies the strength of orientation within a group, and the mean vector (MV), which represents the rank-weighted mean direction of the group. Polar plots display individual vectors, derived from azimuth data collected during the experiment by the encoder at a sampling rate of five times per second, and subsequently analyzed using the Rayleigh test. Each vector representing an individual moth's mean flight direction and directedness (r-value). The vector length reflects the proportion of time a moth maintains a particular direction, ranging from r = 0 (completely un-oriented) to r = 1 (fully oriented). MMRT requires the analysis of each individual's average direction and r-value to determine the group-level mean MV. It is important to note that the magnitude of R^* is dependent on sample size.

To evaluate the directional orientation of moths in different treatment groups, we performed Rayleigh tests on individual flight directions. Subsequently, we used the Friedman test to examine whether different experimental phases within each experiment influenced the r-values of moth orientation, as this test is appropriate for comparing repeated measurements from the same individuals (Table S2). In the initial test, only the Exp. Spring experiment showed significant differences. Therefore, we further compared the flight stability and r-values among its different experimental phases (Table S3). Because r value exhibited non-normal distributions, the Wilcoxon signed-rank test was employed. Since these comparisons involved repeated measurements from the same individuals, pairwise comparisons were conducted. Because multiple comparisons were performed, failing to apply a correction would increase the likelihood of false positives; therefore, the Benjamini–Hochberg procedure was used to control the false discovery rate (FDR).

The Rayleigh r-values for each individual were also used to compare orientation strength across experiment. We accounted for the non-independence between Exp Dark I and Exp Dark II by using the paired Wilcoxon signed-rank test for their pairwise comparison. All other comparisons among independent experiments were performed using the Wilcoxon rank-sum test. The multiple comparisons corrected using the Benjamini-Hochberg procedure to control the false discovery rate (FDR). Detailed statistical results are provided in Table S4.

To evaluate flight stability, we measured the angular difference between consecutive

seconds of recorded flight behavior and calculated the average directional change per second. This metric reflects the consistency and stability of individual flight orientation. Differences among treatment groups were assessed using the Wilcoxon signed-rank test (Table S5) because some of the data did not follow a normal distribution. We also accounted for the non-independence between the Exp Dark I and Exp Dark II experiments, for which paired comparisons were conducted. Multiple comparisons were corrected using the Benjamini–Hochberg procedure to control the false discovery rate (FDR).

Acknowledgements

This work was supported by the National Key Research and Development Program of China (2021YFD1400700), the Fundamental Research Funds for the Central Universities (KJJQ2025013, RENCAI2025031), the Joint Research Program of State Key Laboratory of Agricultural and Forestry Biosecurity (SKLJRP2507) and the National Natural Science Foundation of China to (32202289).

References

Alerstam T, Chapman JW, Bäckman J, Smith AD, Karlsson H, Nilsson C, Reynolds DR, Klaassen RHG, Hill JK, 2011. Convergent patterns of long-distance nocturnal migration in noctuid moths and passerine birds. *Proc. R. Soc. B* **278**:3074-3080. DOI: https://doi.org/10.1098/rspb.2011.0058

Bauer S & Hoye BJ, 2014. Migratory animals couple biodiversity and ecosystem functioning worldwide. *Science* **344**:54-62. DOI: https://doi.org/10.1126/science.1242552

Burda H, Marhold S, Westenberger T, Wiltschko R & Wiltschko W, 1990. Magnetic compass orientation in the subterranean rodent *Cryptomys hottentotus* (Bathyergidae). *Experientia*, *46*(5), 528-530. DOI: https://doi.org/10.1007/BF01954256

Chapman JW, Nesbit RL, Burgin LE, Reynolds DR., Smith AD, Middleton DR, Hill JK. 2010. Flight orientation behaviors promote optimal migration trajectories in high-flying insects. *Science* **327**:682-685. DOI: https://doi.org/10.1126/science.1182990

Chapman JW, Reynolds DR, Wilson K, 2015. Long-range seasonal migration in insects: mechanisms, evolutionary drivers and ecological consequences. *Ecol. Lett.* **18**:287-302. DOI: https://doi.org/10.1111/ele.12407

Chapman JW, Nilsson C, Lim KS, Bäckman J, Reynolds DR, Alerstam T, 2016. Adaptive strategies in nocturnally migrating insects and songbirds: contrasting responses to wind. *J. Anim. Ecol.* **85**:115-124. DOI: https://doi.org/10.1111/1365-2656.12420

Chen H, Wang Y, Huang L, Xu CF, Li JH, Wang FY, Cheng W, Gao BY, Chapman JW, G. Hu, Flight capability and the low temperature threshold of a Chinese field population of the fall armyworm *Spodoptera frugiperda*. *Insects* **13**:422 (2022). DOI: https://doi.org/10.3390/insects13050422

730 Chen H, Wan GJ, Li JC, Ma YB, Reynolds DR, Dreyer D, Warrant EJ, Chapman JW,
731 G. Hu, Adaptive migratory orientation of an invasive pest on a new continent.
732 *iScience* **26**:108281 (2023). DOI: https://doi.org/10.1016/j.isci.2023.1082 81

733 Chen H, Xu CF, Wang YH, Li XR, Yu DH, Chen AD, Lyu BQ, Wu YF, Wang YM,
734 Chapman JW, G. Hu, Characteristics and seasonal variation of fall armyworm
735 migratory behavior in their year-round breeding areas in South China. *Pest Manag.*
736 *Sci.* **81**:4051-4062 (2025). DOI: https://doi.org/10.1002/ps.8772

737 Drake VA & Reynolds DR. 2012. Radar entomology: observing insect flight and
738 migration. Wallingford, UK: CABI

739 Dreyer D, Frost B, Mouritsen H, Günther A, Green K, Whitehouse M, Johnsen S,
740 Heinze S, Warrant E, 2018a. The Earth's magnetic field and visual landmarks
741 steer migratory flight behavior in the nocturnal Australian Bogong moth. *Curr. Biol.*
742 **28**:2160-2166. DOI: https://doi.org/10.1016/j.cub.2018.05.030

743 Dreyer D, el Jundi B, Kishkinev D, Suchentrunk C, Campostrini L, Frost BJ,
744 Zechmeister T, Warrant EJ, 2018b. Evidence for a southward autumn migration of
745 nocturnal noctuid moths in central Europe. *J. Exp. Biol*. **221**:jeb179218. DOI:
746 https://doi.org/10.1242/jeb.179218

747 Dreyer D, Frost B, Mouritsen H, Lefèvre A, Menz M, Warrant EJ, 2021. A guide for
748 using flight simulators to study the sensory basis of long-distance migration in
749 insects. *Front. Behav. Neurosci.* **15**:678936. DOI: https://doi.org/10.3389/fnbeh.
750 2021.678936

751 Dreyer D, Adden A, Chen H, Frost B, H. Mouritsen, J. J. Xu, K. Green, M. Whitehouse,
752 J. Chahl, J. Wallace, G. Hu, J. Foster, S. Heinze, E. J. Warrant, 2025. Bogong
753 moths use a stellar compass for long-distance navigation at night. *Nature*
754 **643**:994-1000. https://doi.org/10.1038/s41586-025-09135-3

755 Engels, S., Schneider, N. L., Lefeldt, N., Hein, C. M., Zapka, M., Michalik, Elbers D.,
756 Kittel A., Hore PJ., Mouritsen, H. Anthropogenic electromagnetic noise disrupts
757 magnetic compass orientation in a migratory bird. *Nature* **509**, 353–356 (2014).
758 https://doi.org/10.1038/nature13290. DOI: https://doi.org/10.1038/nature13290

759 Fleischmann PN, Grob R, Müller VL, Wehner R, Rössler W, 2018. The geomagnetic
760 field is a compass cue in *Cataglyphis* ant navigation. *Curr. Biol*. **28**:1440-1444.
761 DOI: https://doi.org/10.1016/j.cub.2018.03.043

762 Freas CA & Spetch ML, 2023. Varieties of visual navigation in insects. *Anim. Cogn.*
763 **26**:319-342. https://doi.org/10.1016/j.conb.2011.05.020

764 Foster JJ, Smolka J, Nilsson DE, Dacke M, 2018. How animals follow the stars. *Proc.*
765 *R. Soc. B* **285**:20172322. DOI: https://doi.org/10.1098/rspb.2017.2322

766 Fu P, Li X, Sun Z, Chen Y, Lu Z, Tian C, Hu G, Gui F, 2025. Population genetics and
767 trajectory simulation reveals the invasion process of the fall armyworm
768 (*Spodoptera frugiperda*) in the Eastern Hemisphere. *Evol. Appl.* **18**:e70086. DOI:
769 https://doi.org/10.1111/eva.70086

770 Gao BY, Reynolds DR, Zhai BP, Hu G, Chapman JW, 2020. The 'migratory connectivity'
771 concept, and its applicability to insect migrants. *Move. Ecol.* **8**:48. DOI:
772 https://doi.org/10.1073/pnas.2317646121

773 Gao BY, Wotton KR, Hawkes WLS, Menz MHM, Reynolds DR, Zhai BP, Hu G,
774 Chapman JW, 2020. Adaptive strategies of high-flying migratory hoverflies in
775 response to wind currents. *Proc. R. Soc. B* **287**:20200406. DOI:
776 https://doi.org/10.1098/rspb.2020.0406

Gao BY, Reynolds DR, Hu G, Chapman JW, 2024. Effects of nocturnal celestial illumination on high-flying insect migration. *Phil. Trans. Roy. Soc. B* **379**:20230115. DOI: https://doi.org/10.1098/rstb.2023.0115

Gao FQ, Chen H, Kyerematen R, Hu G, Early R, Chapman JW, 2025. High migratory potential of fall armyworm in West Africa despite stable temperatures and widely available year-round habitats. *Insect Sci.* https://doi.org/10.1111/1744-7917.13502 .

Goergen G, Kumar PL, Sankung SB, Togola A, Tamo M, 2016. First report of outbreaks of the fall armyworm *Spodoptera frugiperda* (J E Smith) (Lepidoptera, Noctuidae), a new alien invasive pest in west and central Africa. *PLoS One* **11**:e0165632. DOI: https://doi.org/10.1371/journal.pone.0165632

Goforth KM, Lohmann CMF, Gavin A, Henning R, Harvey A, Hinton TL, Lim DS, Lohmann KJ, 2025. Learned magnetic map cues and two mechanisms of magnetoreception in turtles. *Nature* **638**:1015–1022. DOI: https://doi.org/10.1038/s41586-024-08554-y

Grob R, Wegmann JW, Rössler W, Fleischmann PN, 2024. *Cataglyphis* ants have a polarity-sensitive magnetic compass. *Curr. Biol*. **34**:5833-5838. DOI: https://doi.org/10.1016/j.cub.2024.11.012

R, Farnworth MS, Degen J, Warrant E, Montgomery SH, and el Jundi B, 2025. The diversity of lepidopteran spatial orientation strategies - neuronal mechanisms and emerging challenges in a changing world. *J Comp Physiol A Neuroethol Sens Neural Behav Physiol*. DOI: https://doi.org/10.1007/s00359-025-01780-3.

Guo J, Fu X, Zhao S, Shen X, Wyckhuys KAG, Wu K, 2020. Long-term shifts in abundance of (migratory) crop-feeding and beneficial insect species in northeastern Asia. *J. Pest Sci*. **93**:583-594. DOI: https://doi.org/10.1007/s10340-019-01191-9

Holland RA, Wikelski M, Wilcove DS. 2006, How and why do insects migrate? *Science*, **313**:794-796. https://doi.org/10.1126/science.1127272

Hu G, Lim KS, Horvitz N, Clark SJ, D. R. Reynolds, N. Sapir, J. W. Chapman, Mass seasonal bioflows of high-flying insect migrants. *Science* **354**:1584-1587 (2016). DOI: https://doi.org/10.1126/science.aah4379

Hu G, Feng HQ, Otuka A, Reynolds DR, Drake VA, Chapman JW, 2025. The east Asian Insect flyway: geographical and climatic factors driving migration among diverse crop pests. *Annu. Rev. Entomol*. **70**:1-22. DOI: https://doi.org/10.1146/annurev-ento-012524-124018

Huang JR, Feng HQ, Drake VA, Reynolds DR, Gao BY, Chen FJ, Zhang GY, Zhu J, Gao YB, Zhai BP, Li GP, Tian CH, Huang B, Hu G, Chapman JW, 2024. Massive seasonal high-altitude migrations of nocturnal insects above the agricultural plains of East China. *Proc. Nat. Acad. Sci. USA*. **121**:e2317646121. DOI: https://doi.org/10.1073/pnas.2317646121

Hore PJ, Mouritsen H, 2016. The radical-pair mechanism of magnetoreception. *Annu. Rev. Biophys.* **45**:299-344. DOI: https://doi.org/10.1146/annurev-biophys-032116-094545

Kenis M, Benelli G, Biondi A, Calatayud PA, Day R, Desneux N, Harrison RD, Kriticos D, Rwomushana I, van den Berg J, Verheggen F, Zhang YJ, Agboyi LK, Ahissou RB, Ba MN, Wu KM, 2023. Invasiveness, biology, ecology, and management of the fall armyworm, *Spodoptera frugiperda*. *Entomol. Gen.* **43**:187–241. DOI:

824 https://doi.org/10.1127/entomologia/2022/1659

825 Li XJ, Wu MF, Ma J, Gao BY, Wu QL, Chen AD, Liu J, Jiang YY, Zhai BP, Early R,
826 Chapman JW, Hu G, 2020. Prediction of migratory routes of the invasive fall
827 armyworm in eastern China using a trajectory analytical approach. *Pest Manag.*
828 *Sci.* **76**:454-463. DOI: https://doi.org/10.1002/ps.5530

829 Massy R, Hawkes WLS, Doyle T, Troscianko J, Menz MHM, Roberts NM, Chapman
830 JW, Wotton KR, 2021. Hoverflies use a time-compensated sun compass to
831 orientate during autumn migration. *Proc. R. Soc. B* **288**:20211805. DOI:
832 https://doi.org/10.1098/rspb.2021.1805

833 Menz MHM, Scacco M, Bürki-Spycher HM, Williams HJ, Reynolds DR, Chapman JW,
834 Wikelski M, 2022. Individual tracking reveals long-distance flight-path control in a
835 nocturnally migrating moth. *Science* **377**:764-768. DOI:
836 https://doi.org/10.1126/science.abn166

837 Mouritsen H & Frost B, 2002. Virtual migration in tethered flying monarch butterflies
838 reveals their orientation mechanisms. *Proc. Nat. Acad. Sci. USA*. **99**:10162-10166.
839 DOI: https://doi.org/10.1073/pnas.152137299

840 Mouritsen H, 2018. Long-distance navigation and magnetoreception in migratory
841 animals. *Nature* **558**:50-59. https://doi.org/10.1038/s41586-018-0176-1

842 Nagoshi RN & Meagher RL, 2008. Review of fall armyworm (Lepidoptera: Noctuidae)
843 genetic complexity and migration. *Fla Entomol* **91**:546-554. DOI:
844 https://doi.org/10.1653/0015-4040-91.4.546

845 Pakhomov A, Shapoval A, Shapoval N, and Kishkinev D, 2025. Not all butterflies are
846 monarchs: compass systems in the red admiral (*Vanessa atalanta*), a European
847 diurnal migrant. *bioRxiv*. DOI: https://doi.org/10.1101/2025.05.01.651646

848 Reppert SM, Guerra PA, Merlin C, 2016. Neurobiology of monarch butterfly migration.
849 *Annu. Rev. Entomol.* **61**:25-42. DOI: https://doi.org/10.1146/annurev-ento-
850 010814-020855

851 Srygley RB & Dudley R, 2008. Optimal strategies for insects migrating in the flight
852 boundary layer: Mechanisms and consequences. *Integr. Comp. Biol.* **48**:119-133.
853 DOI: https://doi.org/10.1093/icb/icn011

854 Tay WT, Meagher RL, Czepak C, Groot AT, 2023. *Spodoptera frugiperda*: Ecology,
855 evolution, and management options of an invasive species. *Annu. Rev. Entomol.*
856 **68**:299-317. DOI: https://doi.org/10.1146/annurev-ento-120220-102548

857 Tong DD, Zhang L, Wu NN, Xie DJ, Fang GJ, Coates BS, Sappington TW, Liu YQ,
858 Cheng YX, Xia JX, Jiang XF, Zhan S, 2022. The oriental armyworm genome yields
859 insights into the long-distance migration of noctuid moths. *Cell Rep.* **41**:111843.
860 DOI: https://doi.org/10.1016/j.celrep.2022.111843

861 Wan GJ, Hayden AN, Iiams SE, Merlin C, 2021. Cryptochrome 1 mediates light-
862 dependent inclination magnetosensing in monarch butterflies. *Nat. Comm*. **12**:771.
863 DOI: https://doi.org/10.1038/s41467-021-21002-z

864 Warrant EJ & Dacke M, 2011. Vision and visual navigation in nocturnal insects. *Ann.*
865 *Rev. Entomol.* **56**:239-254. DOI: https://doi.org/10.1146/annurev-ento-120709-
866 144852

867 Warrant EJ, Frost B, Green K, Mouritsen H, Dreyer D, Adden A, Brauburger K, Heinze
868 S, 2016. The Australian Bogong moth *Agrotis infusa*: A long-distance nocturnal
869 navigator. *Front. Behav. Neurosci*. **10**:77. DOI: https://doi.org/10.3389/

fnbeh.2016.00077

Warrant E & Somanathan H, 2022. Colour vision in nocturnal insects. *Philos Trans R Soc Lond B Biol Sci* **377**:20210285. DOI: https://doi.org/10.1098/rstb.2021.0285

Werber Y, Adin E, Chapman JW, Reynolds DR, Sapir N, 2025. Active navigation and meteorological selectivity drive mass intercontinental insect migration patterns through the Levant. *Proc. R. Soc. B* **292**:20250587. DOI: https://doi.org/10.1098/rspb.2025.0587

Westbrook J, Fleischer S, Jairam S, Meagher R, Nagoshi R, 2019. Multigenerational migration of fall armyworm, a pest insect. *Ecosphere* **10**:e02919. DOI: https://doi.org/10.1002/ecs2.2919

Wu QL, Jiang YY, Liu J, Hu G, Wu KM, 2021. Trajectory modeling revealed a southwest-northeast migration corridor for fall armyworm *Spodoptera frugiperda* (Lepidoptera: Noctuidae) emerging from the North China Plain. *Insect Sci*. **28**:649-661. DOI: https://doi.org/10.1111/1744-7917.12852

Wu MF, Qi GJ, Chen H, Ma J, Liu J, Jiang YY, Lee GS, Otuka A, Hu G, 2022. Overseas immigration of fall armyworm, *Spodoptera frugiperda* (Lepidoptera: Noctuidae) invading Korea and Japan in 2019. *Insect Sci.* **29**:505-520. DOI: https://doi.org/10.1111/1744-7917.12940

Satterfield DA, Sillett TS, Chapman JW, Altizer S, Marra PP, 2020. Seasonal insect migrations: massive, influential, and overlooked. *Front. Ecol. Environ.* **18**:335-344. DOI: https://doi.org/10.1002/fee.2217

Sun XX, Hu CX, Jia HR, Wu QL, Shen XJ, Zhao SY, Jiang YY, Wu KM, 2021. Case study on the first immigration of fall armyworm, *Spodoptera frugiperda* invading into China. *J. Integr. Agri.* **20**:664-672. DOI: https://doi.org/10.1016/s2095-3119(19)62839-x

Xu JJ, Pan W, Zhang YC, Li Y, Wan GJ, Chen FJ, Sword GA, Pan WD, 2017. Behavioral evidence for a magnetic sense in the oriental armyworm, *Mythimna separata*. *Biol. Open* **6**:340-347. DOI: https://doi.org/10.1242/bio.022954

Ji Y, Ma YB, Wen ZS, Gao BY, Foster JJ, Yu DH, Wu Y, Wan GJ & Hu, G, 2025. Skyglow-Induced Luminance Gradients Influence Orientation in a Migratory Moth. *Insects*, *16*(12), 1252. DOI: https://doi.org/10.3390/insects16121252

Supplementary information

Table S1. Detailed data of flight orientation behavior assay.

Experiment	period	MV (95% CI lower-upper)	*R**	n	*P* value
Fall Exp. Field	I	183.6 (211-162)	1.76	29	$P < 0.001$
	II	191.0 (235-153)	1.16	29	$0.01 < P < 0.025$
	III	158.1 (316.3-21.2)	0.34	29	$0.5 < P < 0.9$
	IV	354.3 (331.4-27.2)	1.49	29	$0.001 < P < 0.005$
	V	167.7 (191-146)	1.62	29	$P < 0.001$
Spring Exp. Field	I	347.4 (319.5-16.7)	1.59	28	$P < 0.001$
	II	319.1 (351-283)	1.39	28	$0.001 < P < 0.005$
	III	293.7 (33.6-201.3)	0.67	28	$0.1 < P < 0.5$
	IV	245.2 (309.4-193.2)	0.95	28	$0.05 < P < 0.1$
	V	343.8 (326.56-2.92)	1.84	28	$P < 0.001$
Fall Exp. Lab	I	182.9 (203-156)	1.77	27	$P < 0.001$
	II	184.9 (222-153)	1.31	27	$0.005 < P < 0.01$
	III	111.3 (203.9-36.6)	0.69	27	$0.1 < P < 0.5$
	IV	4.1 (350.7-19.3)	2.17	27	$P < 0.001$
	V	137.6 (189.9-94.9)	1.04	27	$0.025 < P < 0.05$
Fall Control	I	180.3 (196-164)	2.10	26	$P < 0.001$
	II	184.1 (199-167)	1.94	26	$P < 0.001$
	III	195.2 (219-160)	1.43	26	$0.001 < P < 0.005$
	IV	6.1 (28.8-340.4)	1.63	26	$P < 0.001$
	V	183.0 (205-162)	1.81	26	$P < 0.001$
Fall Exp. Dark	Control	218.48 (242-187)	1.50	31	$0.001 < P < 0.005$
	Dark	41.03 (178.51-5.31)	0.55	31	$0.1 < P < 0.5$
Exp. BMVC	I	114.51 (277-18.8)	0.32	30	$0.5 < P < 0.9$
	II	215.76 (284-119)	0.65	30	$0.1 < P < 0.5$
	III	105.72 (264.8-13.9)	0.31	30	$0.5 < P < 0.9$
	IV	191.21(284-119)	0.66	30	$0.1 < P < 0.5$

Table S2. Friedman test results of Rayleigh's *r* values across experimental

Experiment	Friedman chi-squared	df	*P* value
Spring Exp. Field	16.207	4	0.002753
Fall Exp. Field	1.1714	4	0.8828
Fall Exp. Lab	8.2154	4	0.084
Fall Control	1.952	4	0.7446

Table S3. Pairwise comparison results of the mean Rayleigh's *r* values of Exp. Spring across different experimental phases, using the Wilcoxon signed rank test with multiple comparison correction performed by the Benjamini-Hochberg method.

Experiment	Comparison group	*P* value	*W* value
Spring Exp. Field	IV-V	0.1545	140
	III-V	0.1545	141
	II-V	0.0519	115
	I-V	0.0021	44
	III-IV	0.9153	184
	II-IV	0.5166	154
	I-IV	0.1545	84
	II-III	0.9153	210
	I-III	0.3691	122
	I-II	0.2615	116

Table S4. Multiple comparisons of mean Rayleigh test *r* values across experimental conditions using the Wilcoxon rank-sum test (adjusted by the Benjamini-Hochberg method).

Comparison	*P* value	*W* value
A vs B	0.32	9084
A vs C	0.01	7632
A vs D	0.54	2407
A vs E	<0.001	3252
A vs F	<0.001	17135
B vs C	0.22	7934
B vs D	0.26	2386
B vs E	<0.001	2958
B vs F	<0.001	15654
C vs D	0.0356	2543
C vs E	<0.001	3186
C vs F	<0.001	16450
D vs E	0.01	400
D vs F	<0.001	3477
E vs F	0.0700	2843

Note: A: Fall Exp. Field; B: Fall Exp. Lab; C: Fall Control; D: Fall Exp. Dark I; E: Fall Exp. Dark II; F: Fall Exp. BMVC.

Table S5. Wilcoxon rank-sum test for mean angular velocity (directional change per second) across experimental conditions, adjusted by the Benjamini-Hochberg method.

Comparison group	*P* value	*W* value
A vs B	0.75	10006
A vs C	0.41	9967
A vs D	0.94	2227
A vs E	0.00	1479
A vs F	0.00	4237
B vs C	0.77	8957
B vs D	0.72	2005
B vs E	0.00	1376
B vs F	0.00	3890
C vs D	0.48	1850
C vs E	0.00	1119
C vs F	0.00	3199
D vs E	0.01	119
D vs F	0.00	929
E vs F	0.02	1332

Note: A: Fall Exp. Field; B: Fall Exp. Lab; C: Fall Control; D: Fall Exp. Dark-I; E: Fall Exp. Dark-II; F: Fall Exp. BMVC.

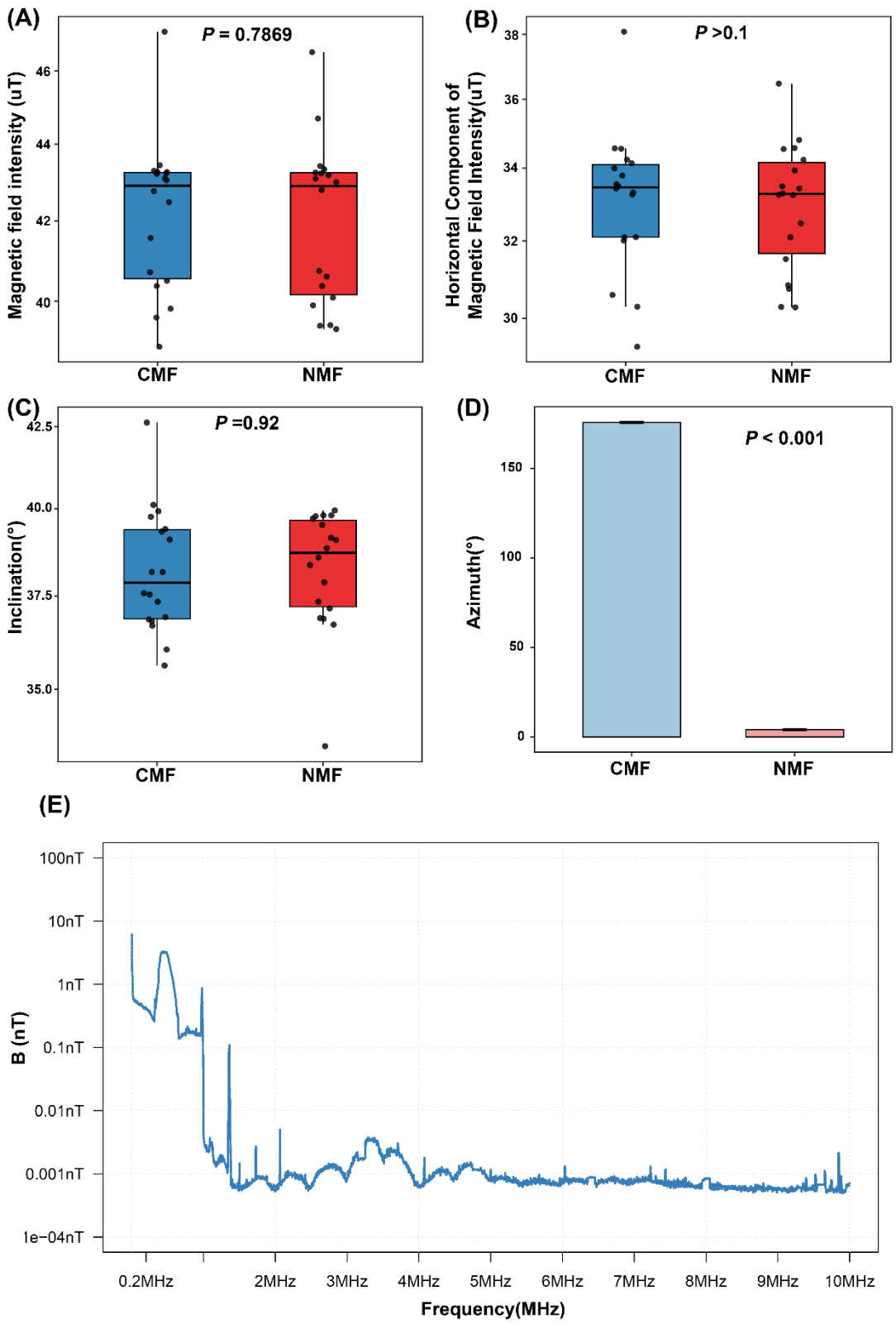

Fig. S1. The magnetic field conditions during experimental procedures in 2023 and 2024. A Comparison of total magnetic field strength between the controlled magnetic field (CMF) and normal magnetic field (NMF) (*t*-test, E_{CMF} = 42.21 μT, E_{NMF} = 42.02 μT, *P* = 0.7869), showing no significant difference. **B** There is no significant

difference in the intensity of the horizontal component between CMF and NMF (*t*-test, H_{CMF} = 31.18, H_{NMF} = 31.35, P >0.1). **C** There is no significant difference in magnetic inclination between CMF and NMF (*Watson-U²*, α_{CMF} = 38.22°, α_{NMF} = 38.28°, P = 0.92). **D** Comparison of magnetic azimuth between CMF and NMF, demonstrating a highly significant difference (*Watson-U²*, β_{CMF} =175.62°, β_{NMF} = 4.11°, P < 0.001). **E** The magnetic component *B*, measured in nanoteslas (nT), of the time-dependent electromagnetic field across a 10 kHz resolution bandwidth (RBW), was analyzed as a function of frequency f, expressed in megahertz (MHz). The data shown in the figure represents the maximum locked values observed over a 40-minute period at the experimental location (23.604°N, 101.977°E). Measurements were conducted using the Spectran NF5035 spectrum analyzer (1 Hz-30 MHz, Aaronia AG), MDF9400 magnetic field antenna (9 kHz-400 MHz, Aaronia AG), UBBV-MDF960X preamplifier (9 kHz-60 MHz, with a gain of 25 dB), and a 10-meter RF cable. The spectrum in the frequency range of 1 MHz to 10 MHz was first measured using the antenna paired with the preamplifier. Subsequently, low-frequency noise within the range of 2 kHz to 1 MHz was detected using the internal probe of the spectrum analyzer. Based on previous studies, electromagnetic noise can, under certain conditions, disrupt the magnetic compass of birds (Engels *et al.*, 2014). Notably, a certain level of noise was present at the low-frequency end (left side of the spectrum) measured in the present study; however, our behavioural results indicate that this level of noise did not completely abolish the contribution of magnetic information to the observed behavioural responses.

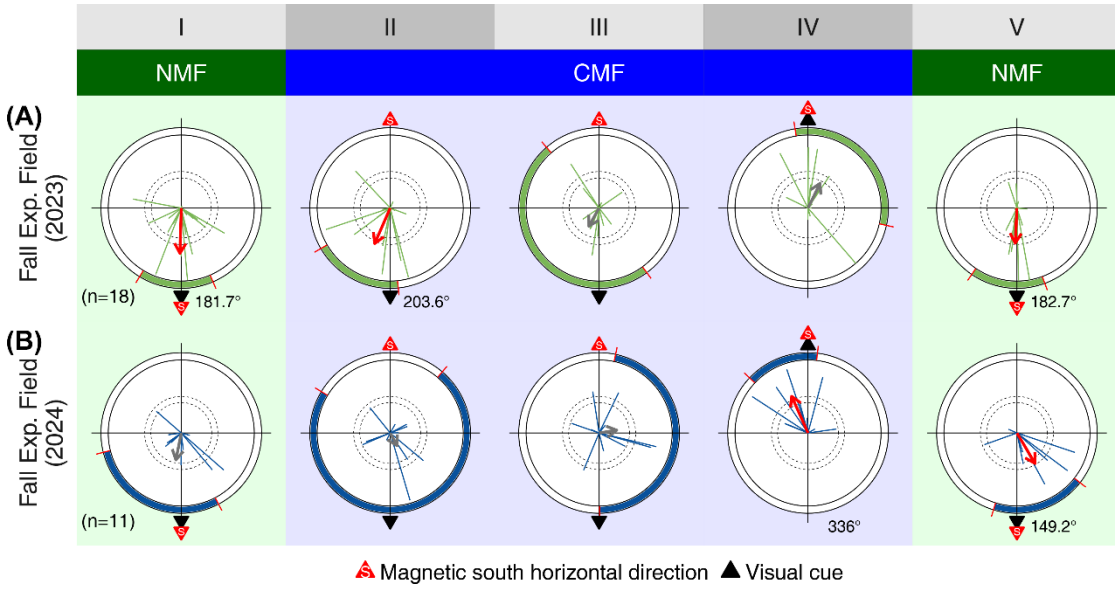

Fig. S2 Year-specific analysis of orientation behavior in field-captured armyworms during the fall migration season (2023 and 2024). A Orientation behavior of the field-captured population in fall 2023. **B** Orientation behavior of the field-captured population in fall 2024. Experiments were conducted using fall armyworms captured from the field, revealing consistent orientation behavior across both years. In both 2023 and 2024, moths oriented significantly toward the visual cue when visual and geomagnetic cues were aligned. However, after reversing the magnetic field, the strength of directional orientation gradually diminished. Due to limited sample sizes in each year, data from both years were pooled for a comprehensive analysis, as presented in Fig. 2B.

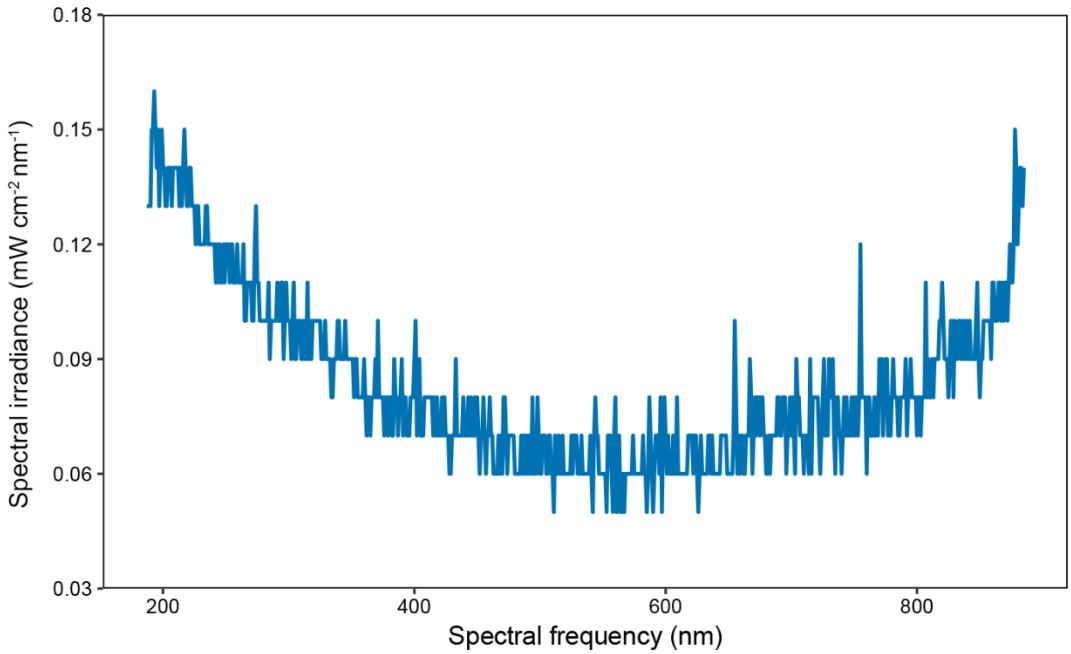

Fig. S3. Spectral distribution of light provided by the full-spectrum lamp. The spectral distribution of the full-spectrum lamp used in the experiment was measured using an ATP2000P spectrometer (Optosky Technology Co. Ltd., Xiamen, China). The sensor was positioned vertically upward at the location originally occupied by the moth's head to measure the spectral irradiance of the light after it passed through the softbox, diffusion paper, and transparent acrylic cover. The results indicate that light radiation was detectable across most wavelengths between 200 nm and 850 nm, confirming that our experimental setup provided a full-spectrum light environment from ultraviolet to near-infrared wavelengths. This spectral range encompasses the known visual sensitivity of moths (Warrant & Somanathan, 2022). Consequently, the acrylic plate and diffusion paper did not significantly block light radiation at any specific wavelength within this range. The ambient light level in the experimental environment was measured to be below 1 lux using a Testo 540 lux meter, manufactured by Testo SE & Co. KGaA (Titisee-Neustadt, Germany).

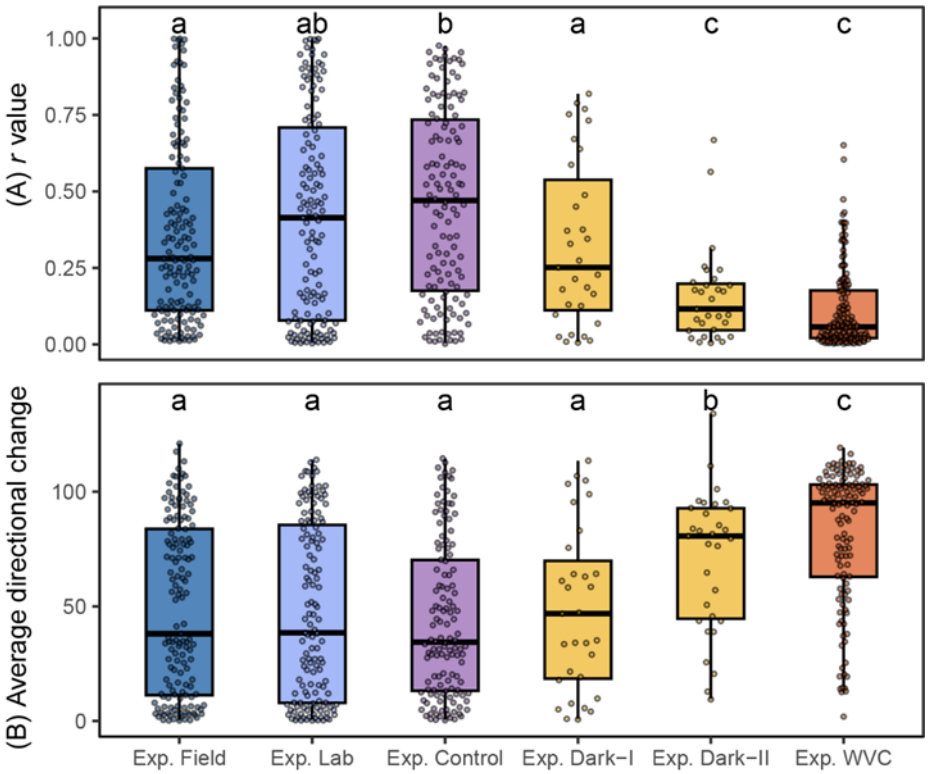

Fig. S4 The lack of visual cues and other necessary visual information significantly affects moth orientation ability and flight stability. A Box plots show the distribution of Rayleigh test *r* values for individual orientations of moths in different treatment groups. **B** Box plots show the distribution of average directional degree change per second, reflecting flight stability, across treatment groups. Boxes represent the interquartile range (IQR), with the horizontal line inside indicating the median. The "whiskers" extend to the most extreme data points within 1.5 times the IQR. Error bars indicate data variability, facilitating comparison between groups. Pairwise comparisons in **A** were conducted using the Wilcoxon rank-sum test with multiple comparisons corrected by the Benjamini-Hochberg method. Detailed statistical results are provided in Supplementary Table S4. In **B**, comparisons were performed using Wilcoxon rank-sum test. Groups labeled with different letters differ significantly ($P < 0.05$). Detailed statistical results are provided in Supplementary Table S5.